Magnetic field specifications for the multipole content of dipole and quadrupole magnets in the 12GeV upgrade

Yves Roblin and Alex Bogacz

Abstract

This note lists the requirements placed upon field inhomogeneities in dipole and quadrupole magnets for the 12 GeV upgrade. These requirements were obtained by using an analytical approach as well as a particle tracking approach. Both methods relied upon placing limits on the induced emittance growth caused by higher order multipoles. Steering and phase space distortion effects were also estimated via tracking. Both studies yielded consistent results. In the remainder of this document we focus on the analytical method. Results are presented in terms of requirements for the flatness of field as well as limits on the coefficients of the multipole expansion in the normal plane.

Introduction

The 12GeV CEBAF upgrade brings a number of unique constraints on the required field quality of the dipoles and quadrupoles magnets. The field non-linearities are sampled across an increased beam size due to the synchrotron radiation. These effects lead to emittance growth, phase-space distortion and transverse kicks. We placed a limit on the magnitude of these non-linearities by using an analytic as well as a particle tracking approach (JLAB-TN-06-029). At that time, the multipole values derived from that note were used for full particle tracking simulations to estimate the effect on the transport and the beam halo (JLAB-TN-06-048). It was shown to be meeting the specifications on transport and halo. This note takes a slightly different approach than in the original estimate from the tracking and provides another way to set the specifications. Future work will involve validating these new specifications via tracking.

Methodology

For a quadrupole, dodecapole (n=5) and icosapole (n=9) are the allowed terms arising from the pole shape and end effects. Errors on the main quadrupole term (n=1) can be factored out from this study since it is generated by roll and DC mis-powering errors and hence can be taken into account in the

misalignment (for the roll) and matching error budgets. The phase space ellipse distortion due to such mismatch will be compensated at each recombiner by matching quadrupoles. On top of these allowed terms, we added random errors and we also included random sextupole (n=2) and octupole (n=3) components to simulate construction errors. In reality, these random components will have a phase angle relative to the mid-plane as well as various rms amplitudes. In the following study we averaged out the phase to express the resulting multipoles in the mid-plane of the magnets. A separate, earlier study based on tracking studied the effect of random versus systematics (JLAB-TN-06-029). Dipoles were allowed an extra sextupole (n=2) and decapole (n=4) term.

In both cases, the criterion for determining the multipole tolerance was based upon observing the relative emittance growth between the ideal field (no multipole) and the field with the non-linearities arising from the multipoles. This mismatch was defined by the ratio between the areas of the new phase-space ellipse encompassing the mismatched beam over the design ellipse. A mismatch per ARC was selected to yield a final emittance growth of no more than 25 % when measured at the entrance of hall D. Because of the energy damping and small synchrotron radiation effects, the first few ARCS have relatively little weight in the final emittance and hence, were allowed a relaxed criterion. The tables below lists the values chosen for the maximum mismatch per ARC for the vertical and horizontal planes assuming decoupled optics.

Segment	Emittance (end of segment)	Emittance with multipole	Fractional growth
ARC1	**4.28E-10**	**6.28E-10**	**0.467**
ARC2	**2.67E-10**	**4.73E-10**	**0.374**
ARC3	**2.19E-10**	**4.58E-10**	**0.457**
ARC4	**2.14E-10**	**4.95E-10**	**0.468**
ARC5	**3.38E-10**	**6.64E-10**	**0.296**
ARC6	**7.46E-10**	**1.12E-09**	**0.134**
ARC7	**1.17E-09**	**1.61E-09**	**0.1**
ARC8	**1.91E-09**	**2.48E-09**	**0.1**
ARC9	**3.55E-09**	**4.42E-09**	**0.1**
ARCA	**5.00E-09**	**6.28E-09**	**0.1**

Table 1 : Allowance for horizontal emittance growth in arcs

Segment	Emittance (end of segment)	Emittance with multipole	Fractional growth

Spr/Rec1	**4.30E-10**	**6.30E-10**	**0.465**
Spr/Rec2	**2.70E-10**	**4.75E-10**	**0.370**
Spr/Rec3	**2.20E-10**	**4.59E-10**	**0.455**
Spr/Rec4	**2.80E-10**	**5.61E-10**	**0.357**
Spr/Rec5	**2.80E-10**	**6.06E-10**	**0.357**
Spr/Rec6	**4.20E-10**	**7.93E-10**	**0.238**
Spr/Rec7	**4.90E-10**	**8.59E-10**	**0.1**
Spr/Rec8	**7.30E-10**	**1.13E-09**	**0.1**
Spr/Rec9	**7.90E-10**	**1.22E-09**	**0.1**
Spr/RecA	**1.13E-09**	**1.63E-09**	**0.1**

Table 2: Allowance for vertical emittance growth in spreaders and recombiners

Field Error Tolerances – Analytic Approach

Analytic formalism describing Courant-Snyder invariant mismatch and the emittance dilution due to magnet field errors (represented by a specific multipole content) has been described in detail in a separate document: JLAB-TN-06-030. Here, we will use Eq. (10-17) from JLAB-TN-06-030 to analyze multipole tolerances for quadrupole and dipole magnets for 12 GeV CEBAF.

To re-cap the analytic formulas, Eq. (10-17); the linear errors, m =1, cause the betatron mismatch – invariant ellipse distortion from the design ellipse without changing its area – no emittance increase.

$$\left(\frac{\sigma_\varepsilon}{\varepsilon}\right)_{mis} = \sqrt{\frac{1}{2}\sum_{n=1}^{N}\left(\beta_n \delta\phi_1\right)^2} = \sqrt{\frac{1}{2}\Delta\phi_1^{\,2}\sum_{n=1}^{N}\left(\beta_n\right)^2_{quad} + \frac{1}{2}\Delta\phi_1^{\,2}\sum_{n=1}^{N}\left(\beta_n\right)^2_{dipole}} \qquad (1)$$

The higher, m > 1, multipoles will contribute to the emittance dilution – 'limited' by design via a separate allowance per each machine segment (Arc). Here one assumes the following multipole content for the dipoles and quads:

- Quads: sextupole (m = 2), octupole (m = 3), duodecapole (m = 5) and icosapole (m = 9)
- Dipoles: sextupole (m = 2) and decapole (m = 4)

Where
$$\left(\frac{\sigma_\varepsilon}{\varepsilon}\right)_{dil} = \sqrt{\frac{1}{2}\sum_{n=1}^{N}\left(\beta_n \Delta\phi\right)^2} = \sqrt{\frac{1}{2}\Delta\phi_{quad}^2\sum_{n=1}^{N}\left(\beta_n\right)_{quad}^2 + \frac{1}{2}\Delta\phi_{dipole}^2\sum_{n=1}^{N}\left(\beta_n\right)_{dipole}^2} \tag{2}$$

$$\Delta\phi_{dipole}^2 = a^2\left[\frac{3}{2}\frac{1}{2^2}(2\times 2)\delta\phi_2{}^2 + 2\frac{5}{2}\frac{1}{2^4}X^{\,2}(2\times 4)\delta\phi_2\delta\phi_4\right] \tag{3a}$$

$$\Delta\phi_{quad}^2 = a^2\left\{\frac{3}{2}\frac{1}{2^2}(2\times 2)\delta\phi_2{}^2 + \frac{5}{2}\frac{1}{2^4}X^{\,2}\left[(3\times 3)\delta\phi_3{}^2 + 2(1\times 5)\Delta\phi_1\delta\phi_5\right]\right\} +$$
$$a^2\left\{\frac{7}{2}\frac{1}{2^6}X_0^4 2(3\times 5)\delta\phi_3\delta\phi_5 + \frac{9}{2}\frac{1}{2^8}X^{\,6}\left[(5\times 5)\delta\phi_5{}^2 + 2(1\times 9)\Delta\phi_1\delta\phi_9\right]\right\} \tag{3b}$$

Here $\phi_n = \dfrac{\int G_n dl}{B\rho} = \int k_n dl$ is the integrated multipole moment in the geometric units, where, one uses multipole expansion coefficients of the azimuthal magnetic field, B_θ, given by the standard Fourier series representation in polar coordinates (at a given point of the r_0 circle):

$$G_m = \frac{1}{r_0^{\,m}}B_{m+1}\ \left[kGauss\ cm^{-m}\right] \qquad k_n = \frac{G_n}{B\rho}\ \left[cm^{-(n+1)}\right] \tag{4}$$

The analytic formalism from JLAB-TN-06-030 allows for the beam trajectory to be perturbed with respect to the design orbit, so that the beam centroid undergoes a betatron oscillation with amplitude X_0 (3 mm) The intrinsic beam size in Eq. (2) is defined as a = 4σ. For details, see Figure 2 in JLAB-TN-06-030.

In case of a quadrupole magnet the magnetic field deviation due to its multipole content from the ideal field at the pole (aperture radius, r) is given by the following expression:

$$\frac{\Delta B}{B} = \sum_{n=2}\frac{\delta\phi_n}{\phi_1^{max}}\ r^{n-1} \tag{5a}$$

For a dipole magnet, similar expression describing the magnetic field deviation due to its multipole content from the ideal field at the half gap, r, can be derived

$$\frac{\Delta B}{B} = \sum_{n=2} \delta\phi_n \; r^n \tag{5b}$$

We make use of the following observation pointed out at CEBAF-TN-0175 and corroborated by DIMAD studies: the field errors due to multipoles of all orders give roughly equal contributions to the relative field error at the pole, ξ;

Quads: $\xi_1 = \frac{\delta\phi_n}{\phi_1^{max}} \; r^{n-1}$ n = 2, (same for all n) (6a)

Dipoles: $\xi_0 = \delta\phi_n \; r^n$ n = 2, (same for all n) (6b)

This allows us to simplify Eq. (3ab) as follows:

$$\Delta\phi_{quad} = \phi_1^{\max} \xi_1 \frac{a}{R_1} \tag{7a}$$

$$\Delta\phi_{dipole} = \xi_0 \frac{a}{R_0^2} \tag{7b}$$

Where

$$\frac{1}{R_1} = \frac{1}{r}\sqrt{\frac{3}{2}\frac{1}{2^2}(2\times 2) + \frac{5}{2}\frac{1}{2^4}\left(\frac{X}{r}\right)^2 (3\times 3) + \frac{7}{2}\frac{1}{2^6}\left(\frac{X}{r}\right)^4 2(3\times 5) + \frac{9}{2}\frac{1}{2^8}\left(\frac{X}{r}\right)^8 (5\times 5) + O\left(\frac{\Delta\phi_1}{\phi_1^{\max}}\right)} \tag{8a}$$

$$\frac{1}{R_0^2} = \frac{1}{r^2}\sqrt{\frac{3}{2}\frac{1}{2^2}(2\times 2) + \frac{5}{2}\frac{1}{2^4}\left(\frac{X}{r}\right)^2 (2\times 4)} \tag{8a}$$

The last term in Eq. (8a), originating from $\Delta\phi_1\delta\phi_n$ cross terms in Eq. (3a), is much smaller than the rest of the expression and therefore can be neglected (the value of $\Delta\phi_1$ is set by an independent C-S invariant tolerance; see Eq. (1)).

Assuming certain allowed emittance dilution $\left(\frac{\sigma_\varepsilon}{\varepsilon}\right)_{dil}$ or a given machine section one can evaluate ξs using Eq. (2)

$$\xi_1 = \frac{\frac{R_1}{a}\left(\frac{\sigma_\varepsilon}{\varepsilon}\right)_{dil}}{\phi_1^{\max}\sqrt{\frac{1}{2}\sum_{n=1}^{N}(\beta_n)^2_{quad}}} \qquad \xi_0 = \frac{\frac{R_0^2}{a}\left(\frac{\sigma_\varepsilon}{\varepsilon}\right)_{dil}}{\sqrt{\frac{1}{2}\sum_{n=1}^{N}(\beta_n)^2_{dipole}}} \tag{9ab}$$

Then the corresponding multipoles can be written as follows:

Quads:
$$\delta\phi_n = \frac{\xi_1\phi_1^{max}}{r^{n-1}} = \frac{\frac{R_1}{a}\left(\frac{\sigma_\varepsilon}{\varepsilon}\right)_{dil}}{r^{n-1}\sqrt{\frac{1}{2}\sum_{n=1}^{N}(\beta_n)^2_{quad}}} \tag{10a}$$

Dipoles:
$$\delta\phi_n = \frac{\xi_0}{r^n} = \frac{\frac{R_0^2}{a}\left(\frac{\sigma_\varepsilon}{\varepsilon}\right)_{dil}}{r^n\sqrt{\frac{1}{2}\sum_{n=1}^{N}(\beta_n)^2_{dipole}}} \tag{10b}$$

Magnet Tolerances for 12 GeV CEBAF Lattice

The limits on 'tolerable' magnet errors will be set in terms of specific allowances for the betatron mismatch (10% increase) and emittance dilution (different allowance set for different Arcs, see appropriate column $\left(\frac{\sigma_\varepsilon}{\varepsilon}\right)_{dil}$ in Tables 1-4).

The linear errors, focusing (m =1), cause the betatron mismatch (invariant ellipse distortion from the design) without emittance increase. The sources of the betatron mismatch come from the quad gradient errors and the dipole body gradients (to be compensated by the dedicated matching quads)

The higher, m > 1, multipoles will contribute to the emittance dilution – 'limited' by design via a separate allowance.

Using Arc 1-10 optics (summarized for the arcs proper in JLAB-TN-06-030 and for the Spr/Rec in JLAB-TN-07-017) one can evaluate Eq. (1) and (2) for each segment. Table 1-2 (quads) and Table 3-4 (dipoles) summarize focusing error tolerances and field quality specs – higher multipoles for groups of quads and dipoles in the corresponding arcs (including the arc proper and Spr/Rec sections). The values of multipoles calculated via Eq. (10ab) (for specific emittance dilution allowance in a given arc) are collected in the tables below.

Conversion to engineering units

Using the multipole values given in the tables, one can express the field non-linearity B'L/BL in terms of the distance x from the trajectory. For dipole magnets, the equations are given below for the spreader and recombiner dipoles in table 3 and the arc dipoles in table 4. The first column gives the dimensionless ratio

BCOM	ΔBL/BL equation	B'L/BL equation (m-1)
1S	(15*X**2+9E4*X**4)/18.58*360.0/π	(30*X+36E4*X**3)/18.58*360.0/π
2S	(4.0*X**2+2.5E4*X**4)/10.80*360.0/π	(8.0*X+10E4*X**3)/10.80*360.0/π
3S	(5.8*X**2+3.6E4*X**4)/6.54*360.0/π	(11.6*X+14.4E4*X**3)/6.54*360.0/π
4S	(3.1*X**2+1.9E4*X**4)/5.52*360.0/π	(6.2*X+7.6E4*X**3)/5.52*360.0/π
5S	(2.5*X**2+1.5E4*X**4)/3.97*360.0/π	(5*X+6E4*X**3)/3.97*360.0/π
6S	(0.39*X**2+2400*X**4)/3.71*360.0/π	(0.78*X+9600*X**3)/3.71*360.0/π
7S	(0.14*X**2+880*X**4)/2.85*360.0/π	(0.28*X+3520*X**3)/2.85*360.0/π
8S	(0.13X**2+800*X**4)/2.80*360.0/π	(0.26X+3200*X**3)/2.80*360.0/π
9S	(0.031*X**2+190*X**4)/2.23*360.0/π	(0.062*X+760*X**3)/2.23*360.0/π
AS	(0.044*X**2+270*X**4)/2.24*360.0/π	(0.088*X+1080*X**3)/2.24*360.0/π

Table 3: Variation of B'L/BL and ΔBL/BL along transverse dimension for dipole magnets in spreader/recombiners

Arc	ΔBL/BL equation	B'L/BL equation (m-1)
MBE 1A	(8.1*X**2+5.0E4*X**4)*16/π	(16.2*X*+20.0E4*X**3)*16/π
MBR 2A	(5.4*X**2+3.4E4*X**4)*16/π	(10.8*X+13.6E4*X**3)*16/π
MBE 3A	(8.0*X**2+5.0E4*X**4)*32/π	(16*X+20.0E4*X**3)*32/π
MBB 4A	(8.0*X**2+5.0E4*X**4*32/π	(16*X+20.0E4*X**3)*32/π
MBB 5A	(3.9*X**2+2.4E4*X**4)*32/π	(7.8*X+9.6E4*X**3)*32/π
MBB 6A	(1.8*X**2+1.1E4*X**4)*32/π	(3.6*X+4.4E4*X**3)*32/π
MBA 7A	(0.76*X**2+4700*X**4)*32/π	(1.52*X+18800*X**3)*32/π

MBA 8A	(0.80X**2+5000*X**4)*32/π	(1.6*X+20000*X**3)*32/π
MBA 9A	(0.43*X**2+2700*X**4)*32/π	(0.86*X+10800*X**3)*32/π
MBA AA	(0.37*X**2+2300*X**4)*32/π	(0.74*X+9200*X**3)*32/π

Table 4: Variation of B'L/BL and ΔBL/BL along transverse dimension for dipole magnets in Arcs

, the second column gives the ratio (ΔB/Δx) L/BL where we set B'=ΔB/Δx in the notations. This B'L/BL ratio is in units of inverse meters. In these equations, x is in units of meters and the multipoles are in units of inverse powers of meters. These equations are shown on figure 1 and 2 for the first BCOM magnet for the SW and NE spreaders. The equations were obtained by dividing the ΔBL polynomial expansion by the integrated nominal field B_0L which, when combined with bρ ($b\rho/B_0L$) gives the bending angle appearing in the equations. Figure 3 and 4 show the same thing for the arc dipoles.

For quadrupole magnets, a similar approach can be used but this time one normalizes to the integrated quadrupole field ($B_1L(x) = k_1Lx$). Alternatively one can express the ratio of the field gradient error over the total quadrupole gradient G'/G2. These results are summarized in tables 5 and 6.

ARC quads	ΔBL/B_1Lx equation (dimensionless)	G'/G2 (dimensionless)
MQB1A	(0.62*x**1+23*X**2+3.2E4*x**4+5.9E10*x**8)/0.32	(1.24*x**1+69*X**2+1.6E5*x**4+5.3E11*x**8)/0.32
MQC2A	(0.42*X**1+14*x**2+1.9E4*x**4+3.7E10*x**8)/0.37	(0.84*X**1+42*x**2+9.5E4*x**4+1.85E11*x**8)/0.37
MQA3A	(0.57*X**1+40*x**2+1.9E5*x**4+4.6E12*x**8)/0.31	(1.14*X**1+120*x**2+9.5E5*x**4+4.14E13*x**8)/0.31
MQA 4A	(0.52*X**1+36*x**2+1.8E5*x**4+4.2E12*x**8)/0.30	(1.04*X**1+108*x**2+9E5*x**4+3.78E13*x**8)/0.30
MQA 5A	(0.25*X**1+18*x**2+8.6E4*x**4+2.0E12*x**8)/0.32	(0.50*X**1+54*x**2+4.3E5*x**4+1.8E13*x**8)/0.32
MQA 6A	(0.16*X**1+11*x**2+5.5E4*x**4+1.3E12*x**8)/0.31	(0.32*X**1+33*x**2+2.75E5*x**4+1.17E13*x**8)/0.31

MQA 7A	(0.081*X**1+5.7*x**2+2.8E4*x**4+6.6E11*x**8)/0.33	(0.162*X**1+17.1*x**2+1.4E5*x**4+5.94E12*x**8)/0.33
MQA 8A	(0.071*X**1+4.9*x**2+2.4E4*x**4+5.8E11*x**8)/0.31	(0.142*X**1+14.7*x**2+1.2E5*x**4+5.22E12x**8)/0.31
MQA 9A	(0.046*X**1+3.2*x**2+1.6E4*x**4+3.8E11*x**8)/0.33	(0.092*X**1+9.6*x**2+8.0E4*x**4+3.42E12*x**8)/0.33
MQPAA	(0.039*X**1+2.7*x**2+1.3E4*x**4+3.2E11*x**8)/0.33	(0.078*X**1+8.1*x**2+6.5E4*x**4+2.88E12*x**8)/0.33

Table 5: Variation of $\Delta BL/B_1Lx$ and G'/G2 across transverse dimension X for quadrupoles in arcs

ARC quads	$\Delta BL/B_1Lx$ equation (dimensionless)	G'/G2 (dimensionless)
MQB1S	(0.56*X**1+21*X**2+2.8E4*X**4+5.3E10*X**8)/0.44	(1.12*X**1+63*X**2+1.4E5*X**4+4.77E11*X**8)/0.44
MQC2S	(0.16*X**1+5.9*X**2+8.2E3*X**4+1.5E10*X**8)/0.75	(0.32*X**1+17.7*X**2+4.1E4*X**4+1.35E11*X**8)/0.75
MQA3S	(0.31*X**1+21*X**2+1.0E5*X**4+2.5E12*X**8)/0.49	(0.62*X**1+63*X**2+5.0E5*X**4+2.25E13*X**8)/0.49
MQA4S	(0.61*X**1+43*X**2+2.1E5*X**4+5.0E12*X**8)/0.58	(1.22*X**1+129*X**2+1.05E6*X**4+4.5E13*X**8)/0.58
MQA5S	(0.29*X**1+20*X**2+1.0E5*X**4+2.4E12*X**8)/0.55	(0.58*X**1+60*X**2+5.0E5*X**4+2.16E13*X**8)/0.55

MQA6S	(0.051*X**1+3.5*X**2+1.7E4*X**4+4.1E11*X**8)/0.59	(0.102*X**1+10.5*X**2+8.5E4*X**4+3.69E12*X**8)/0.59
MQA7S	(0.018*X**1+1.3*X**2+6.3E3*X**4+1.5E11*X**8)/0.56	(0.036*X**1+3.9*X**2+3.15E4*X**4+1.35E12*X**8)/0.56
MQA8S	(9.5E3*X**1+0.67*X**2+3.3E3*X**4+7.8E10*X**8)/0.47	(1.9E4*X**1+2.01*X**2+1.65E4*X**4+7.02E11*X**8)/0.47
MQA9S	(0.011*X**1+0.78*X**2+3.8E3*X**4+9.1E10*X**8)/0.21	(0.022*X**1+2.34*X**2+1.9E4*X**4+9.1E10*X**8)/0.21
MQAAS	(0.011*X**1+0.77*X**2+3.8E3*X**4+9.0E10*X**8)/0.46	(0.022*X**1+2.31*X**2+1.9E4*X**4+9.0E10*X**8)/0.46

Table 6: Variation of $\Delta BL/B_1Lx$ and G'/G2 across transverse dimension X for quadrupoles in arcs

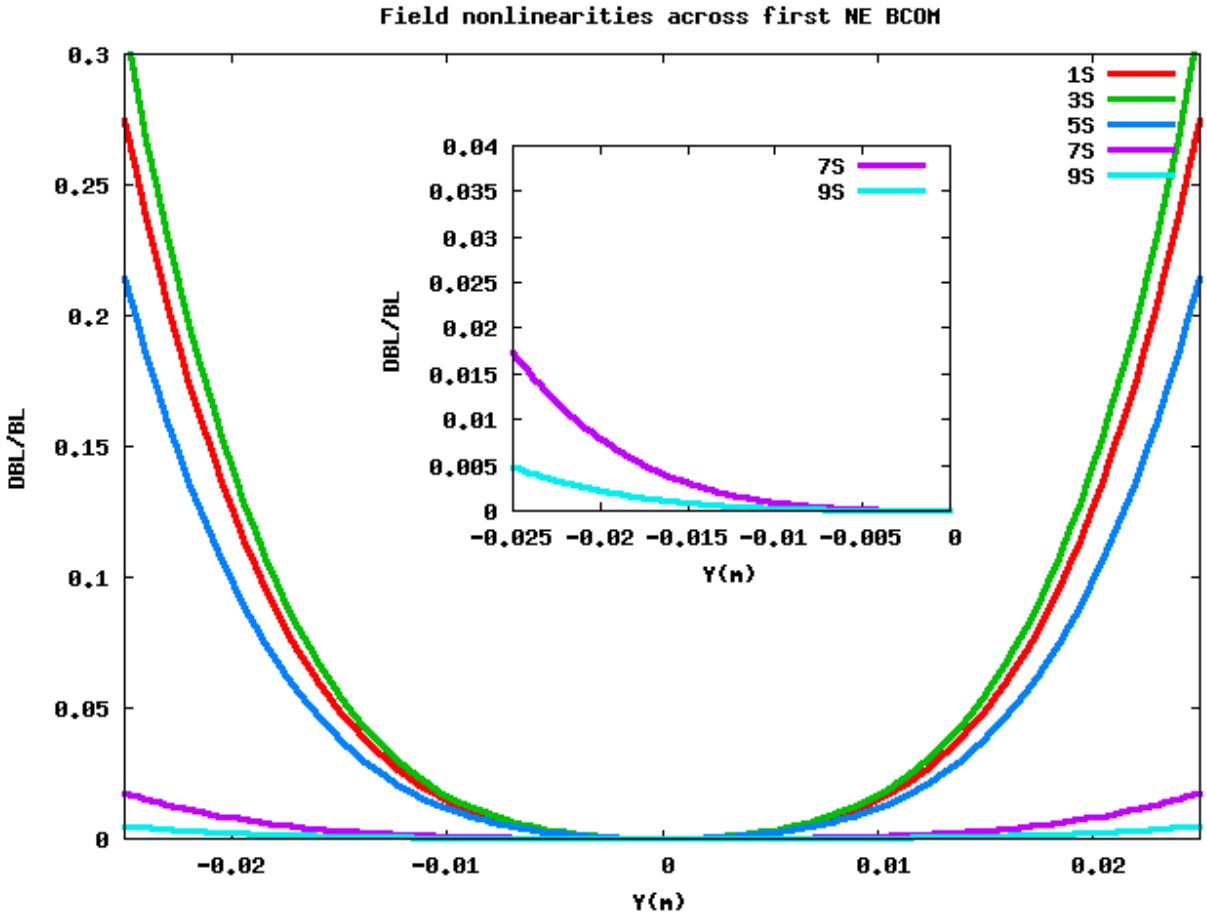

Figure 1: ΔBL/BL Field non linearities across first NE BCOM

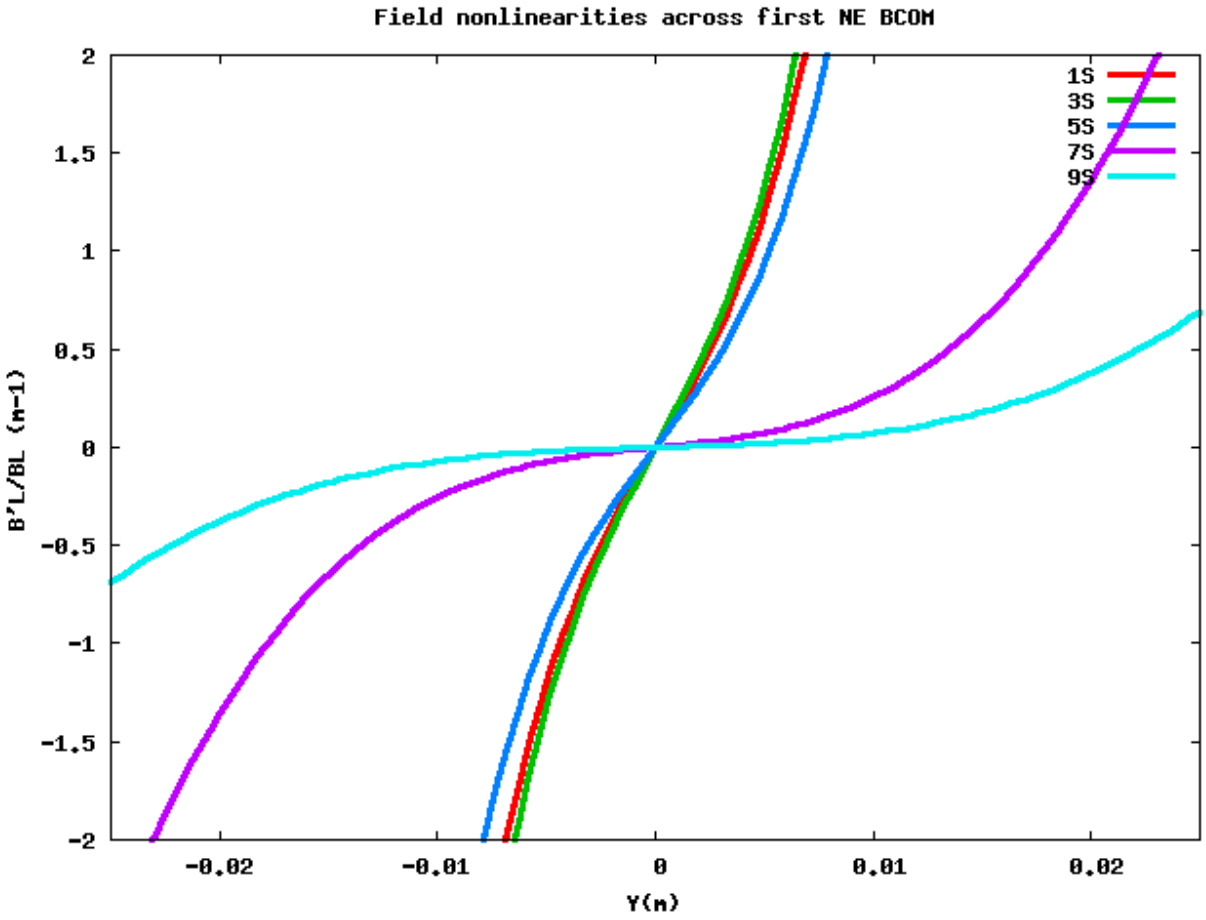

Figure 2: B'L/BL Field non linearity for NE BCOM

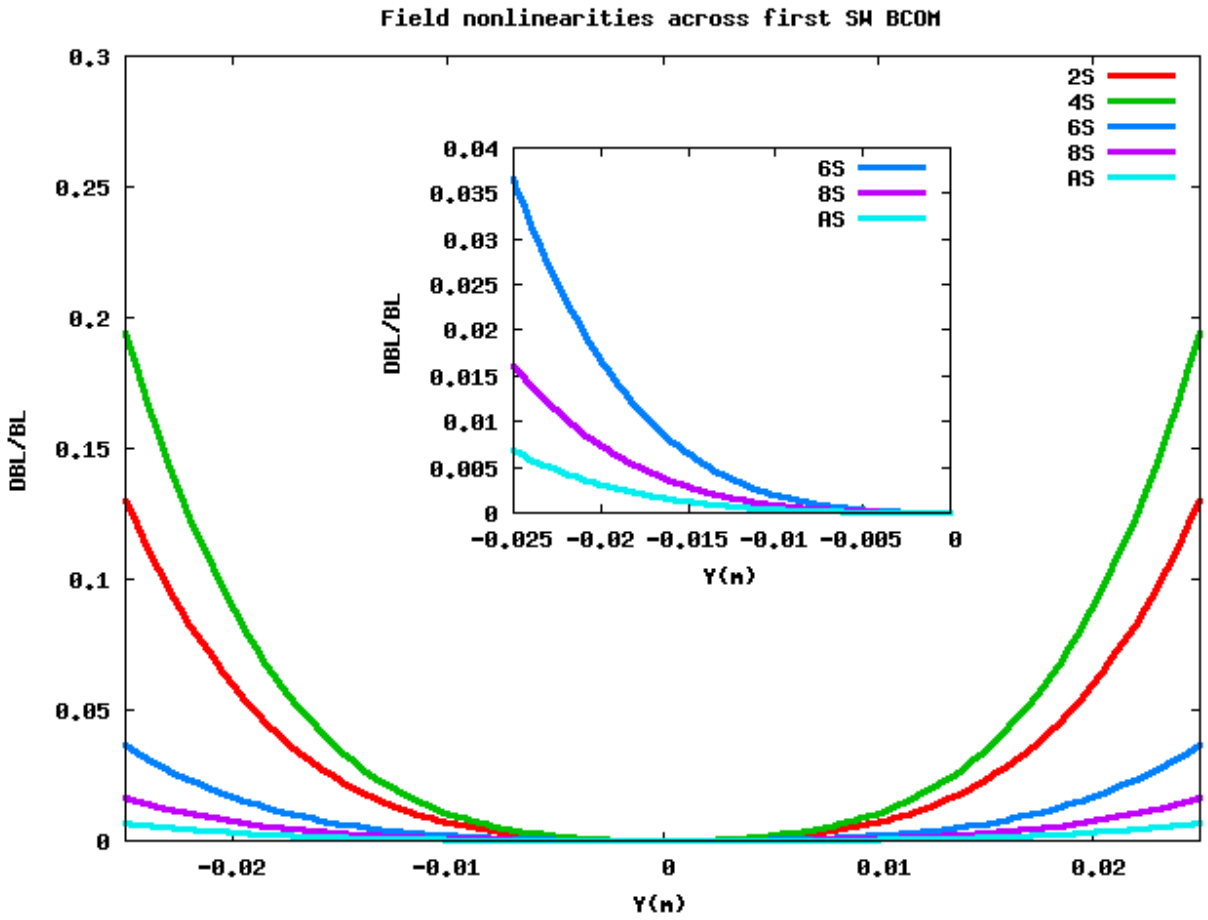

Figure 3: ΔBL/BL Field non linearities across first SW BCOM

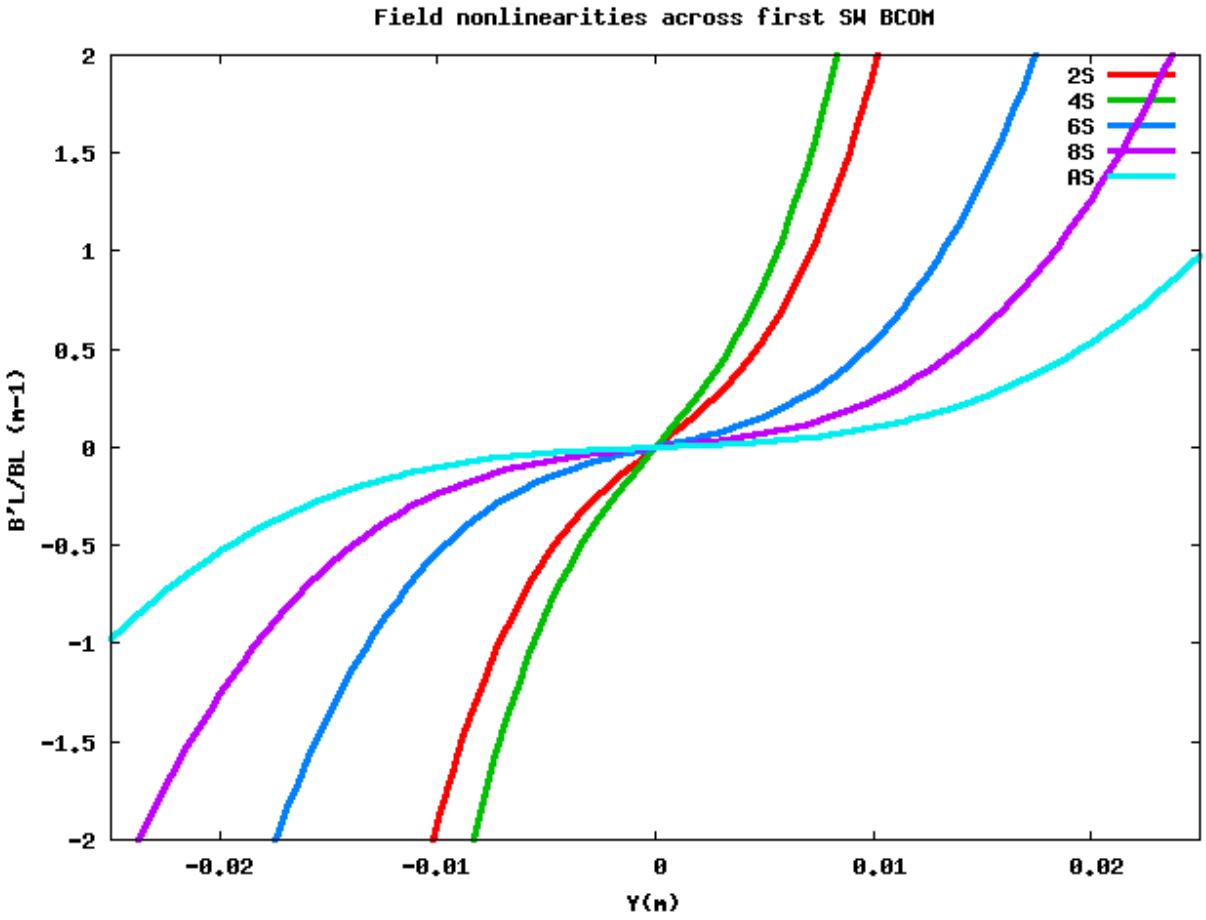

Figure 4: B'L/BL field non linearity across first SW BCOM

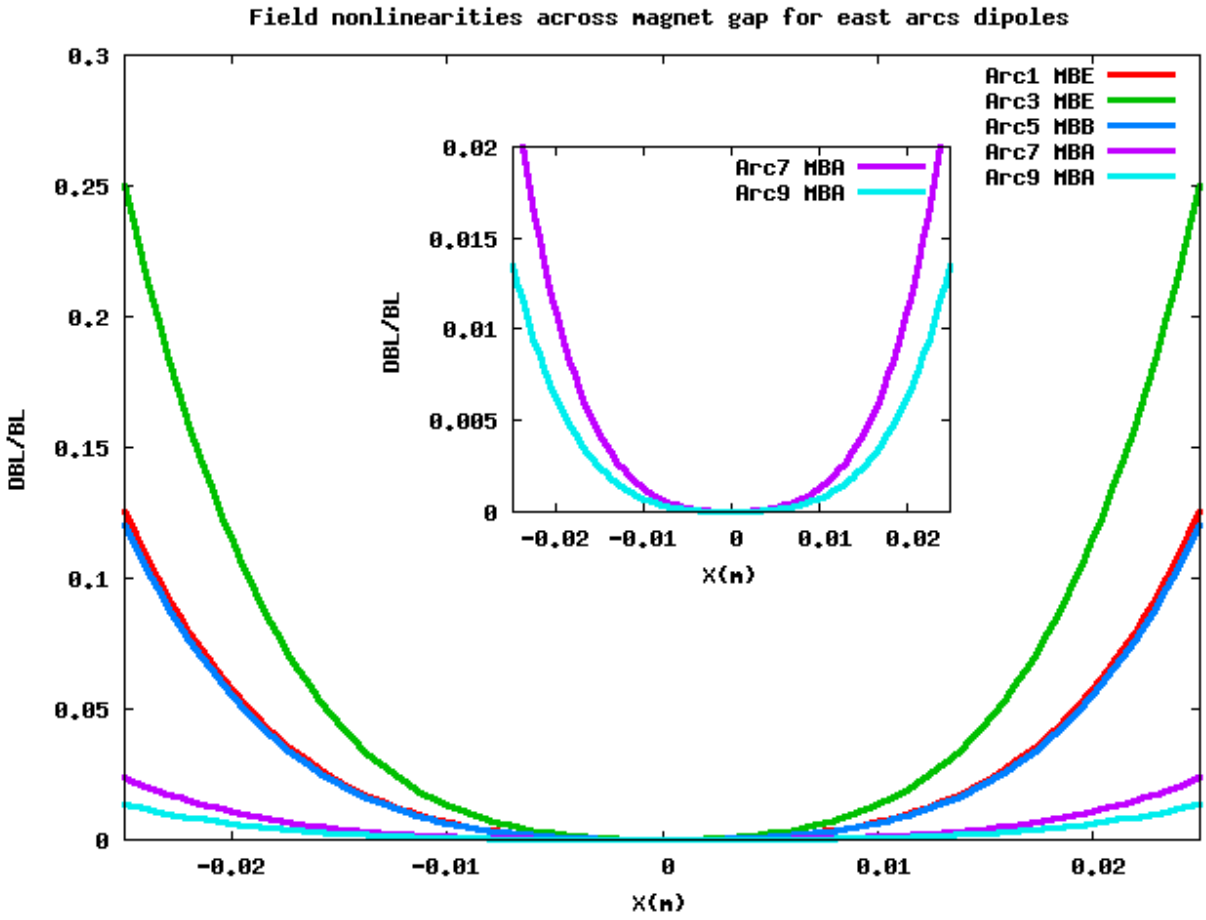

Figure 5: ΔBL/BL Field non linearities across magnet gap for east arcs dipoles

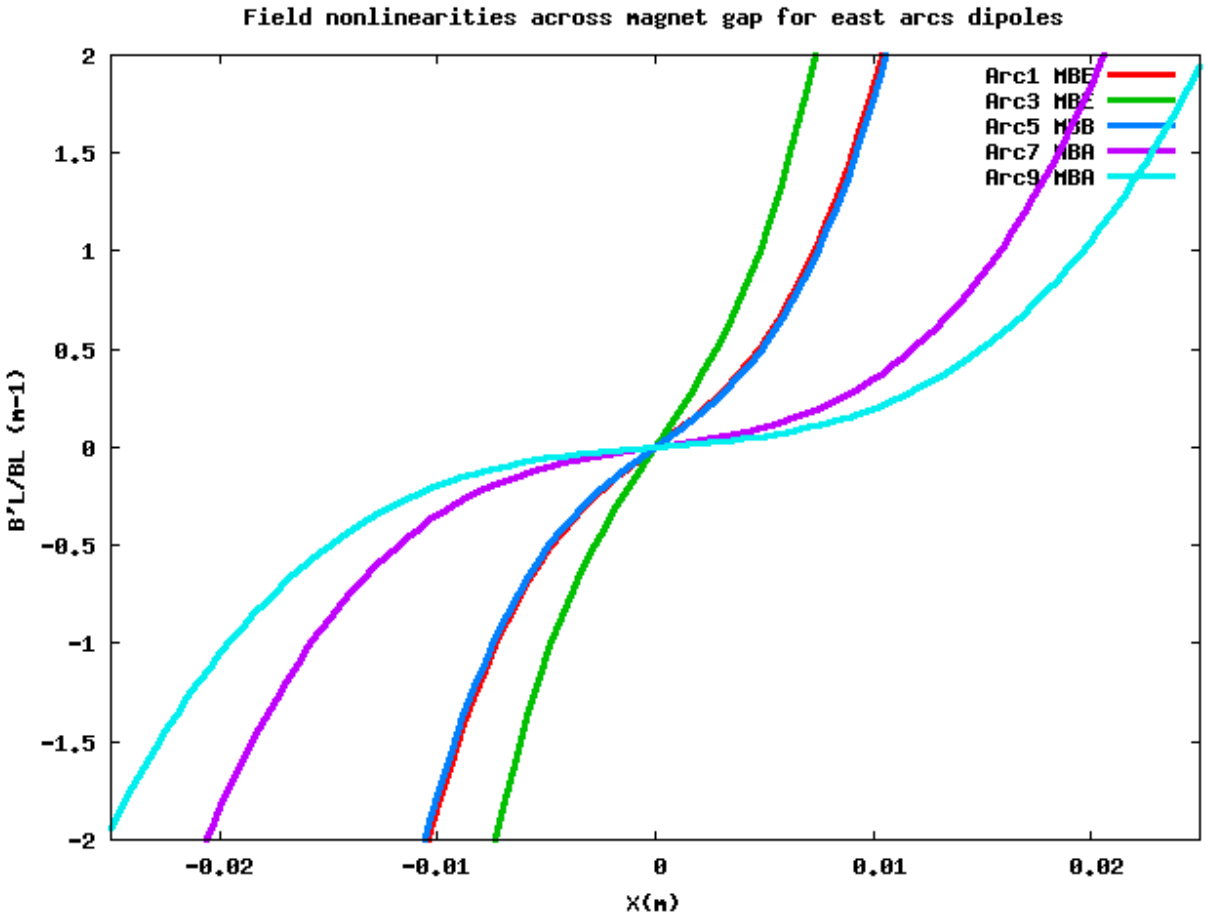

Figure 6: B'L/BL field non linearity for east arc dipoles

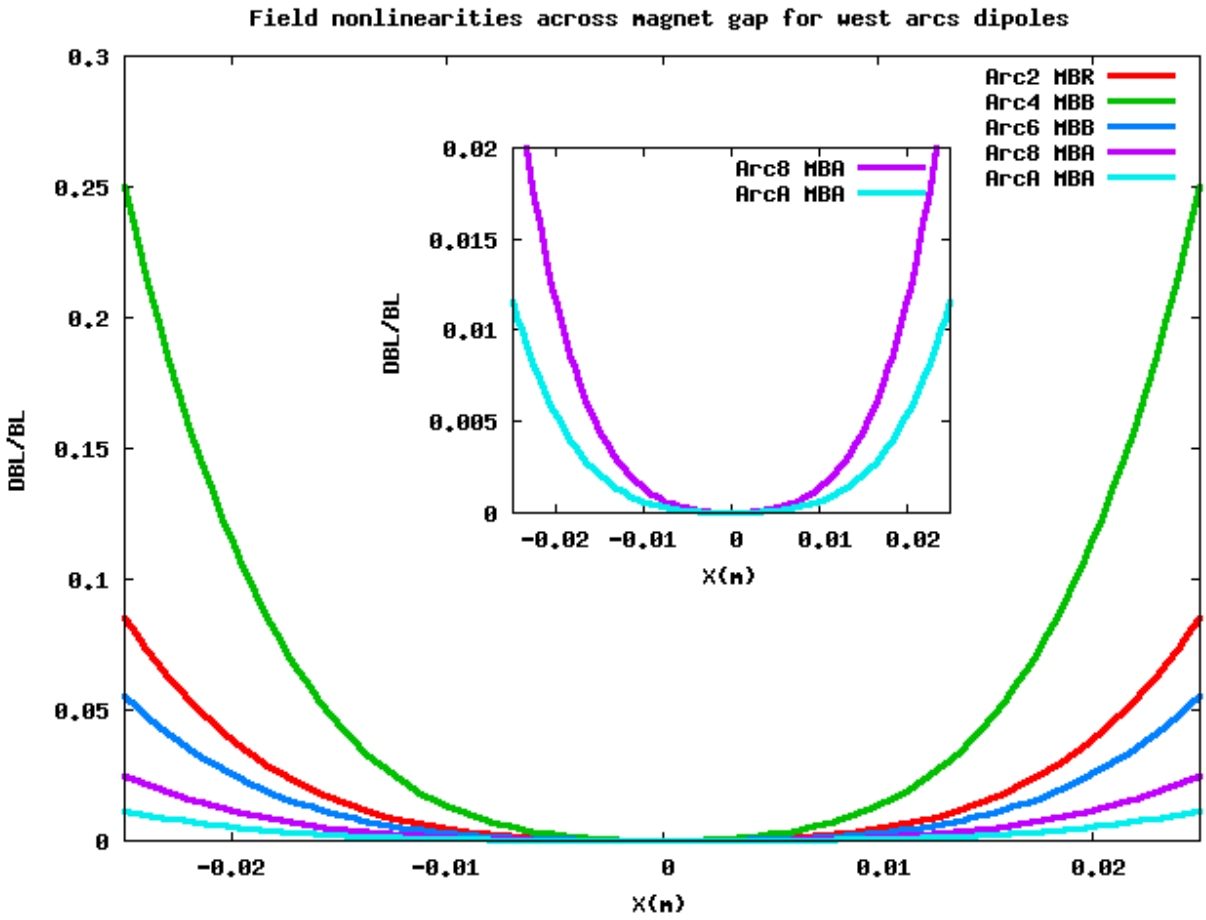

Figure 7: ΔBL/BL Field non linearities across magnet gap for west arc dipoles

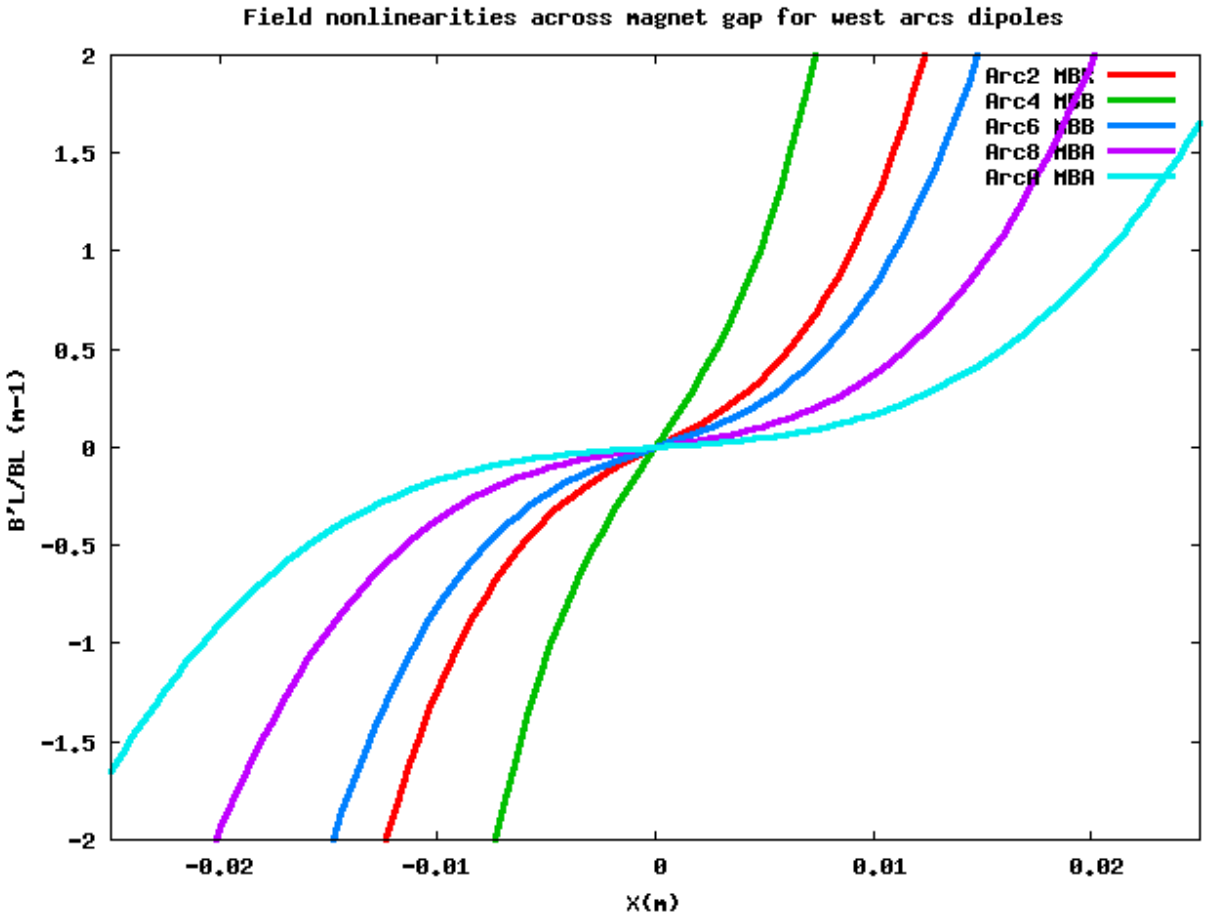

Figure 8: B'L/BL field non linearity across west arc dipoles

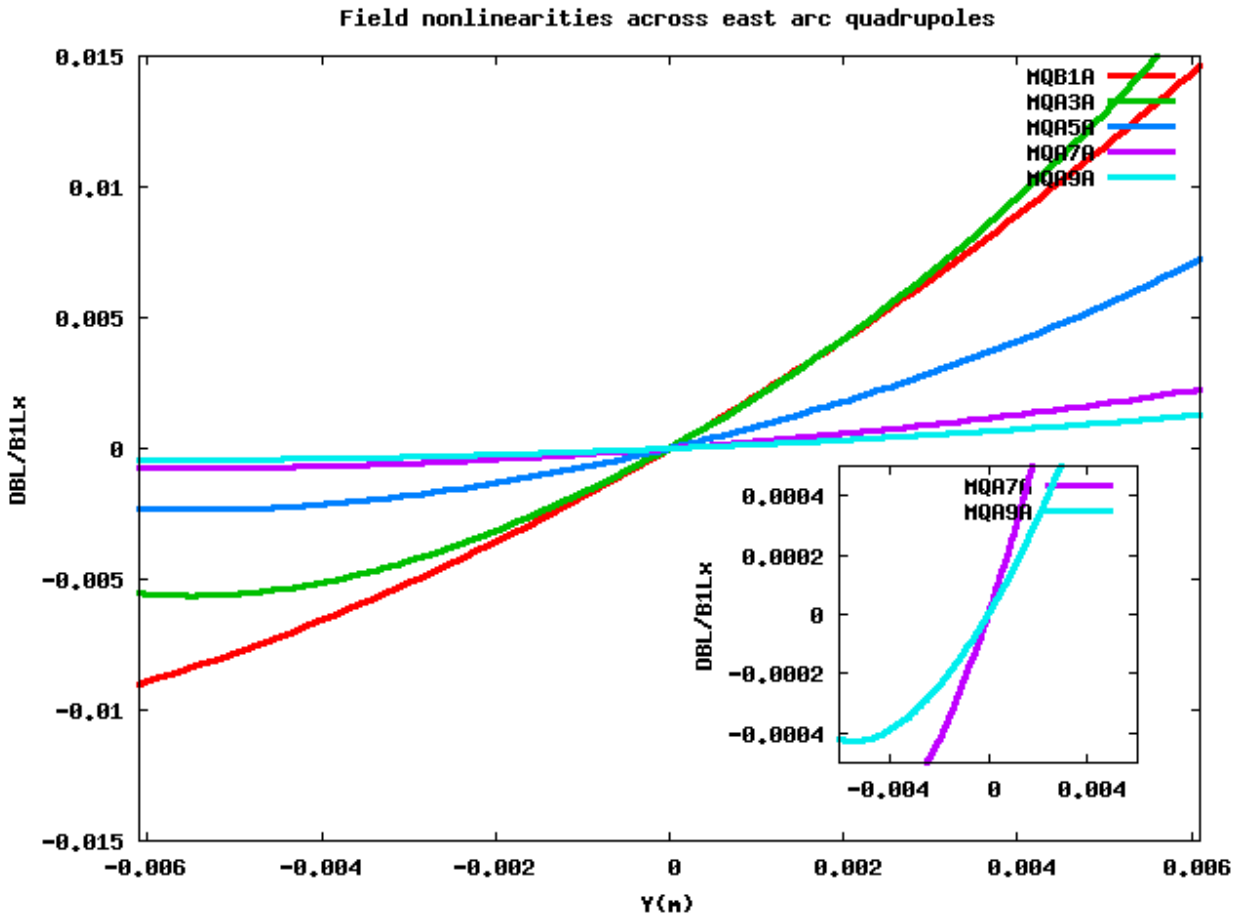

Figure 9: Field non linearities across east arcs quadrupoles

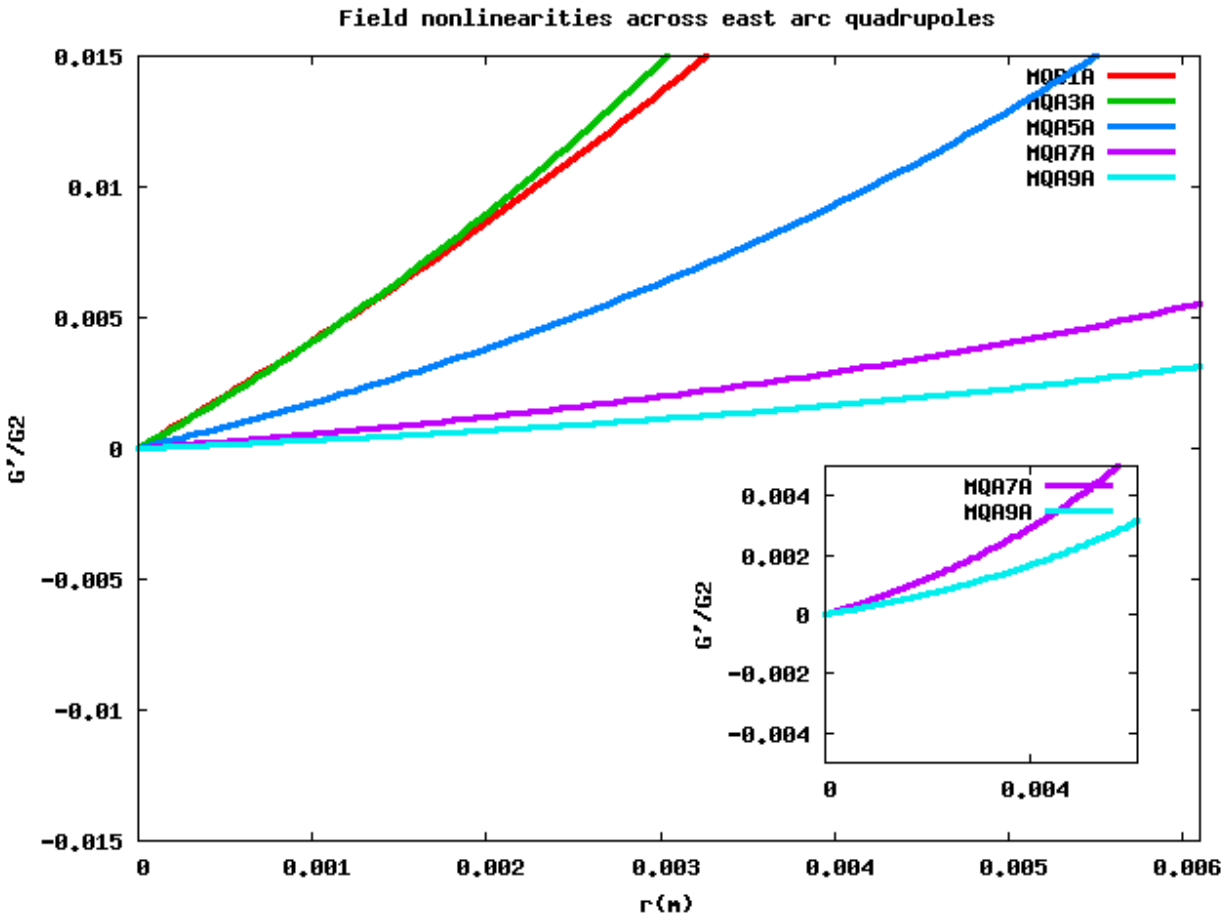

Figure 10: G'/G2 gradient ratio across transverse dimension for east arc quadrupoles

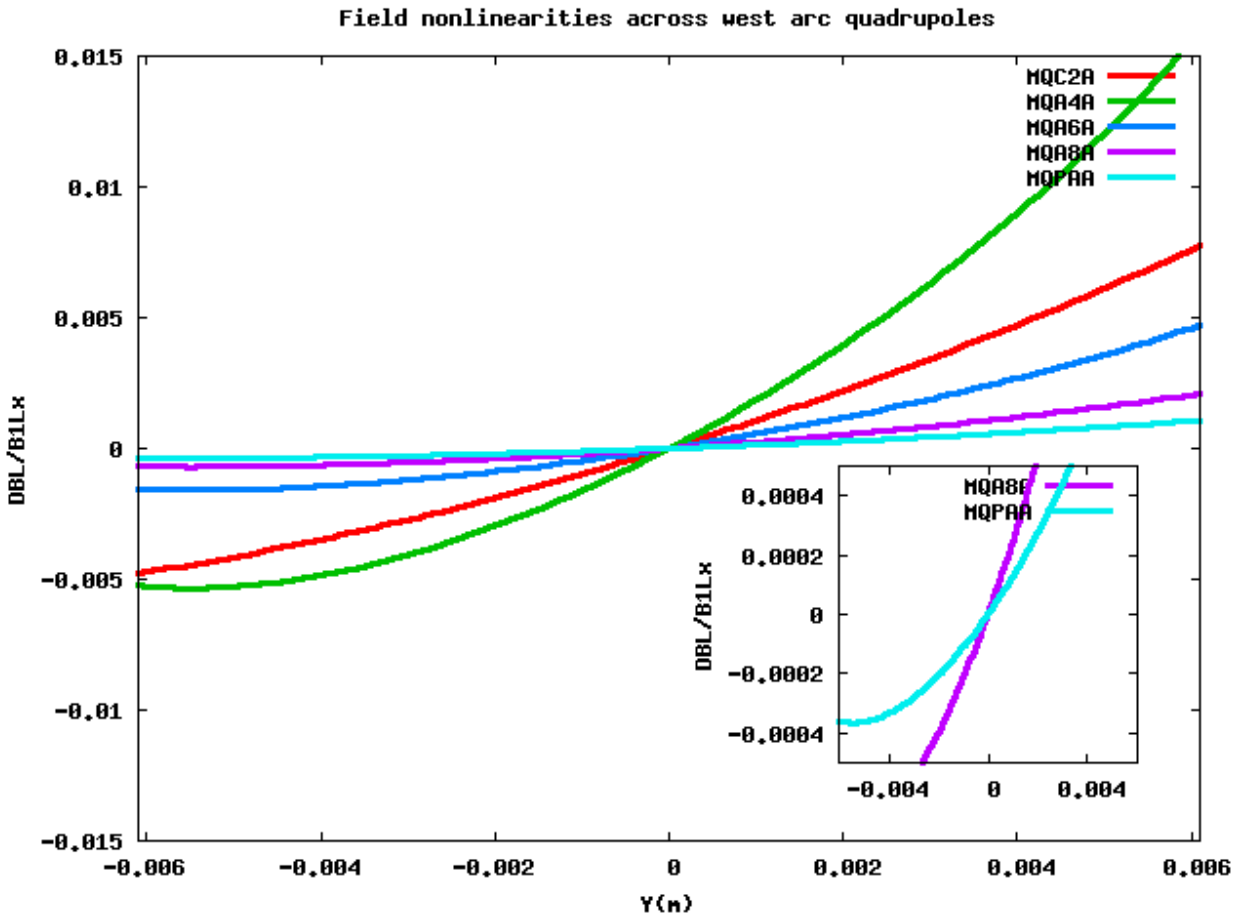

Figure 11: Field non linearities across west arcs quadrupoles

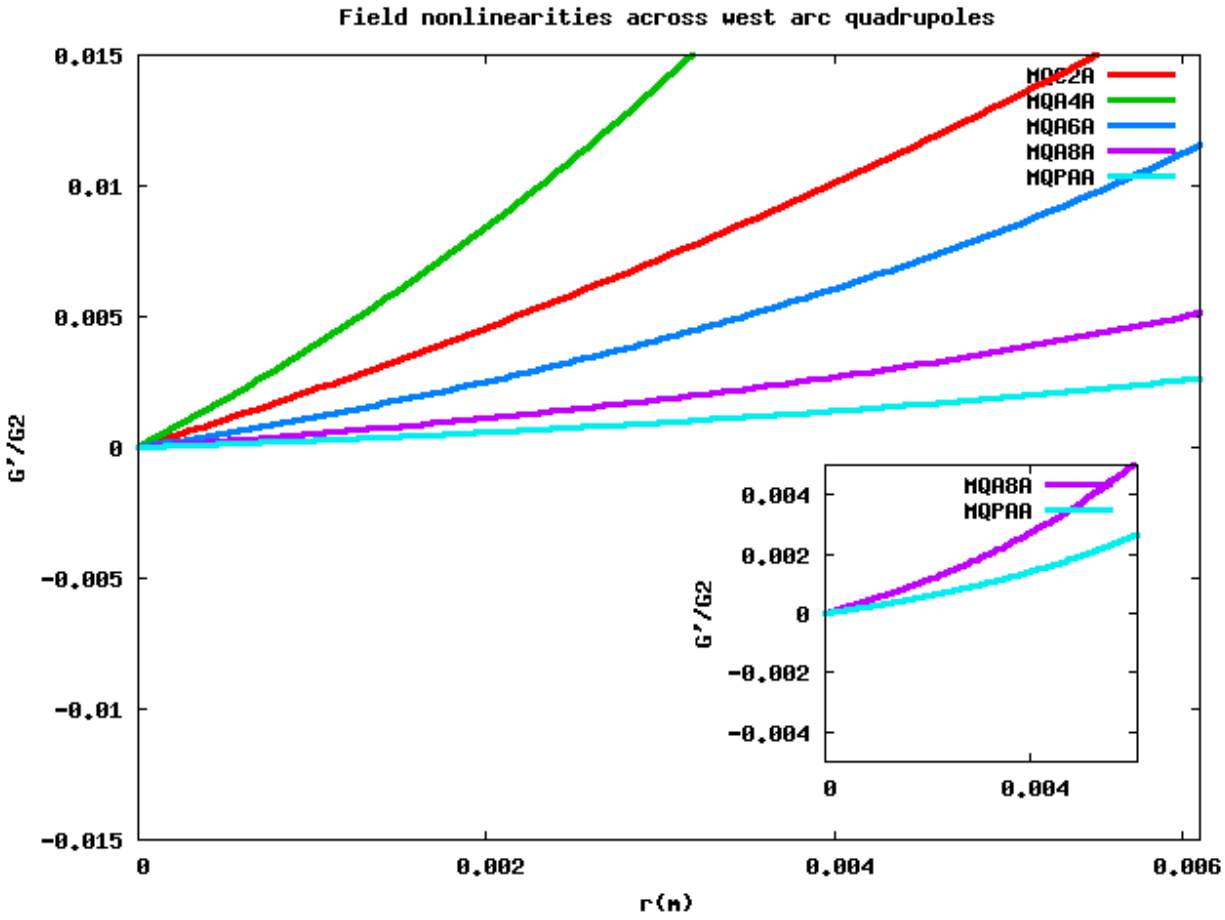

Figure 12: G'/G2 gradient ratio across west arc quadrupoles

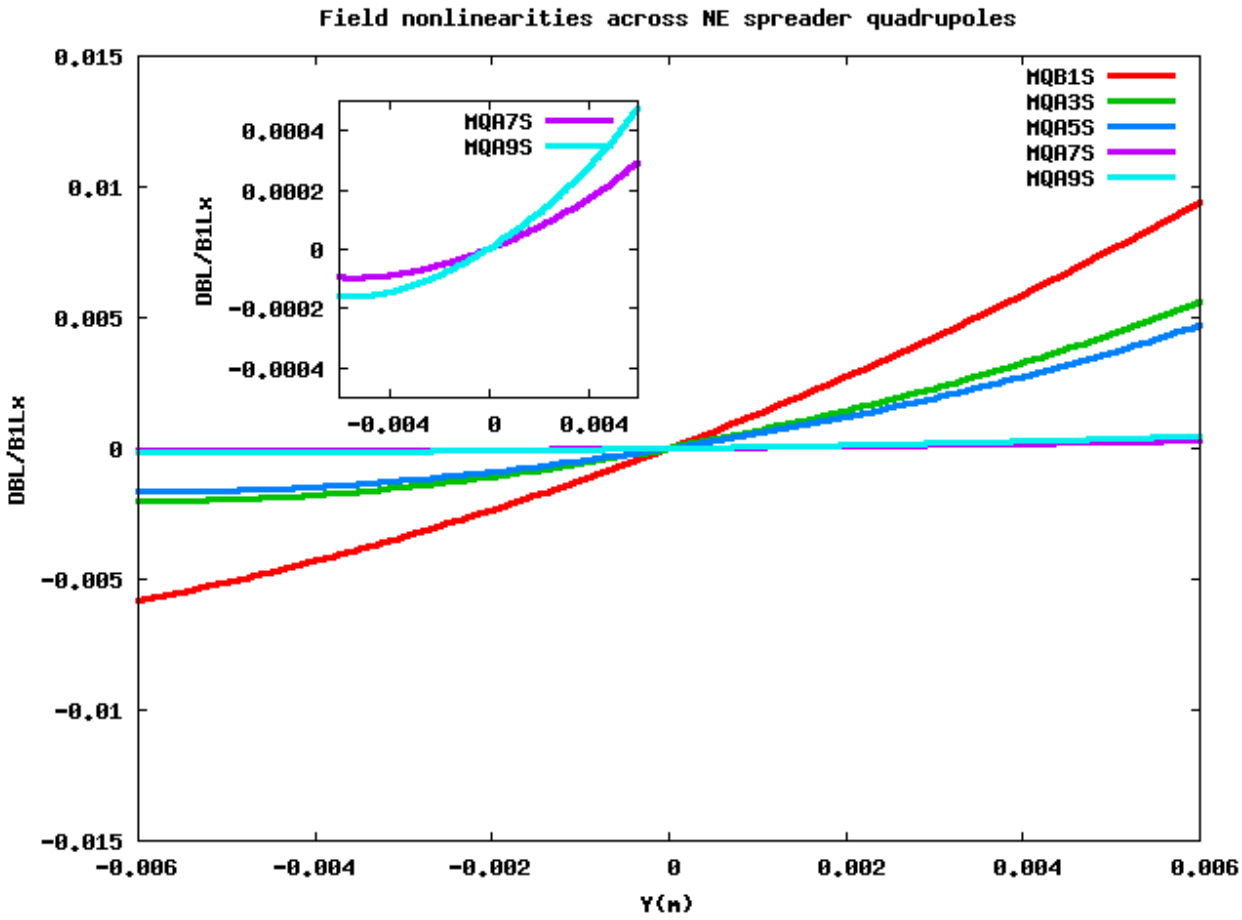

Figure 13: Field non linearities across NE spreader quadrupoles

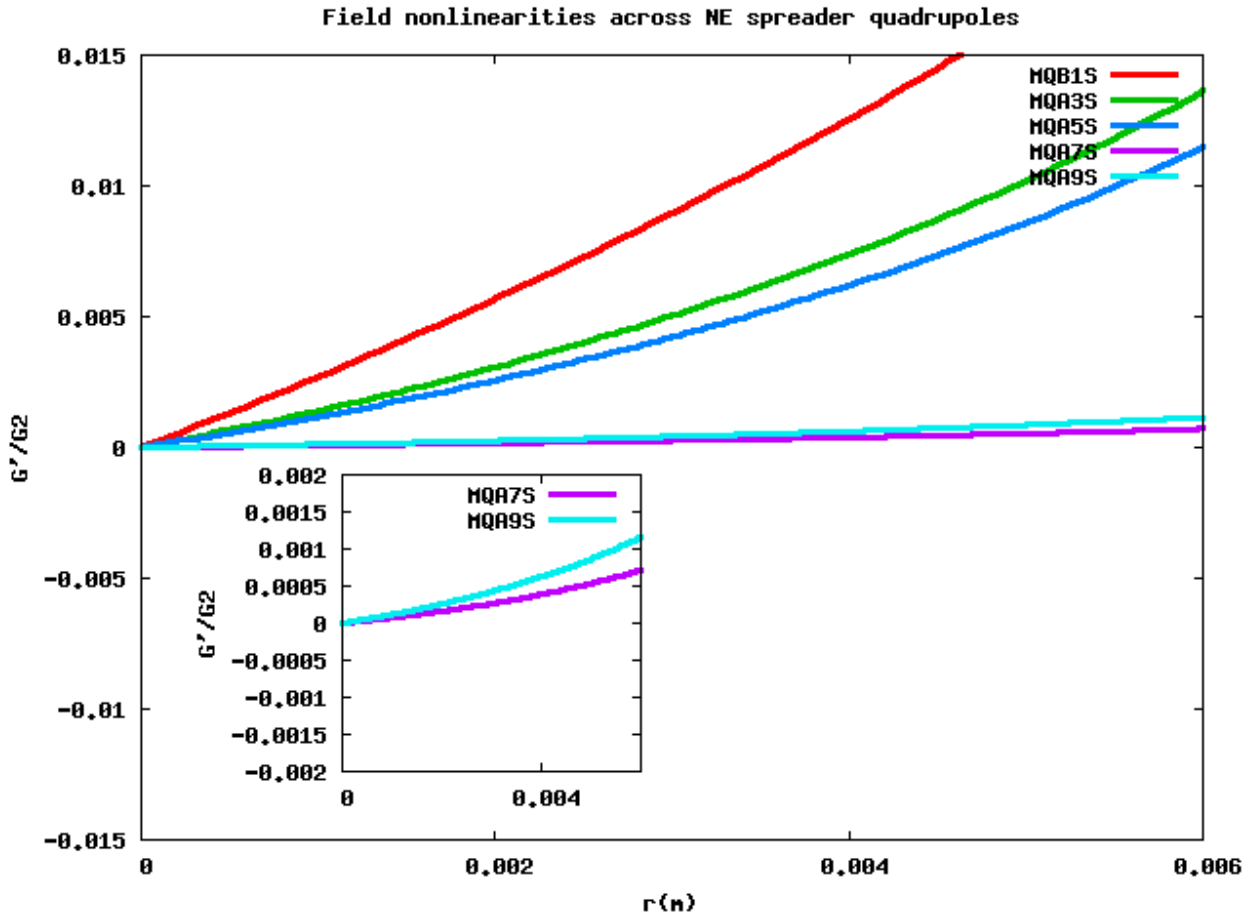

Figure 14: G'/G2 gradient ratio across NE spreader quadrupoles

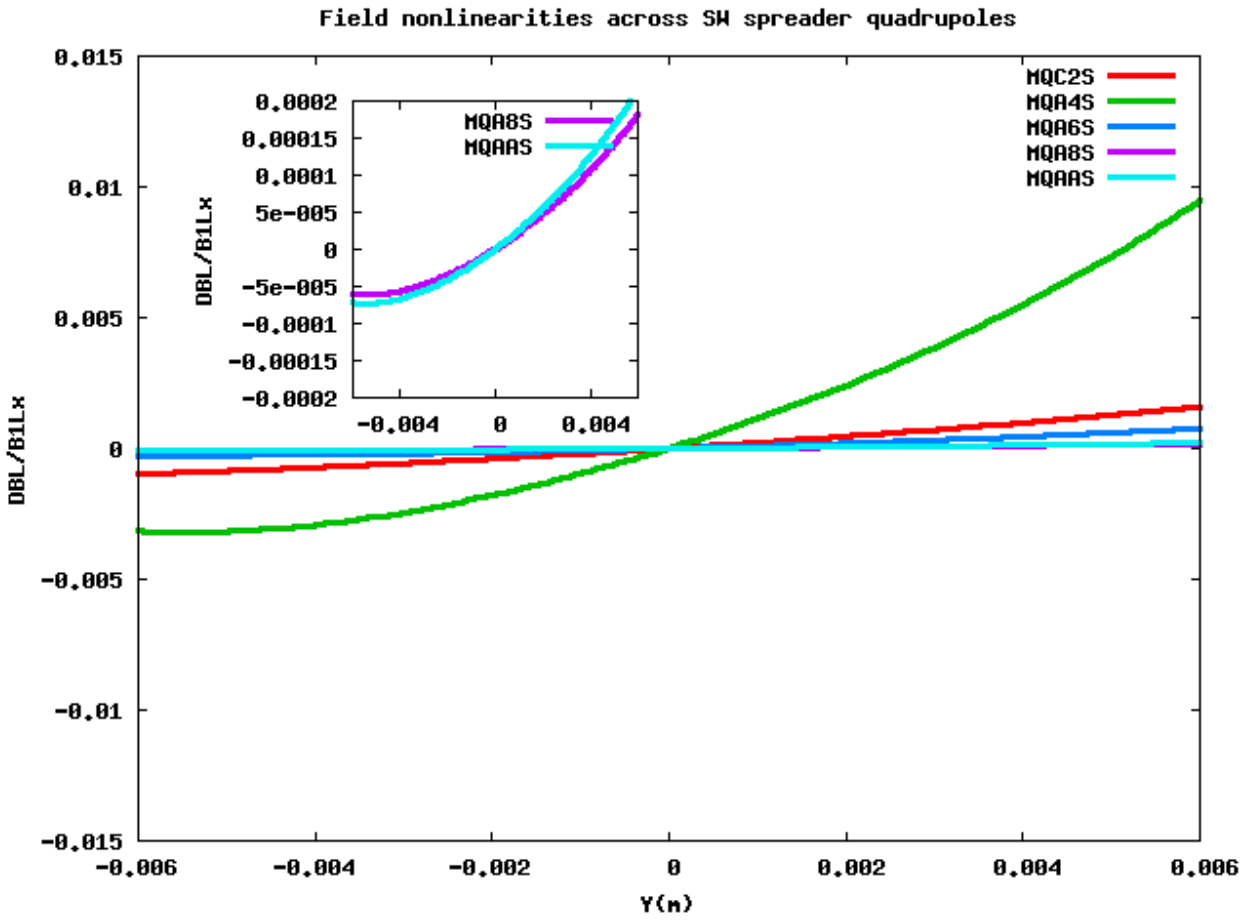

Figure 15: Field non linearities across SW spreader quadrupoles

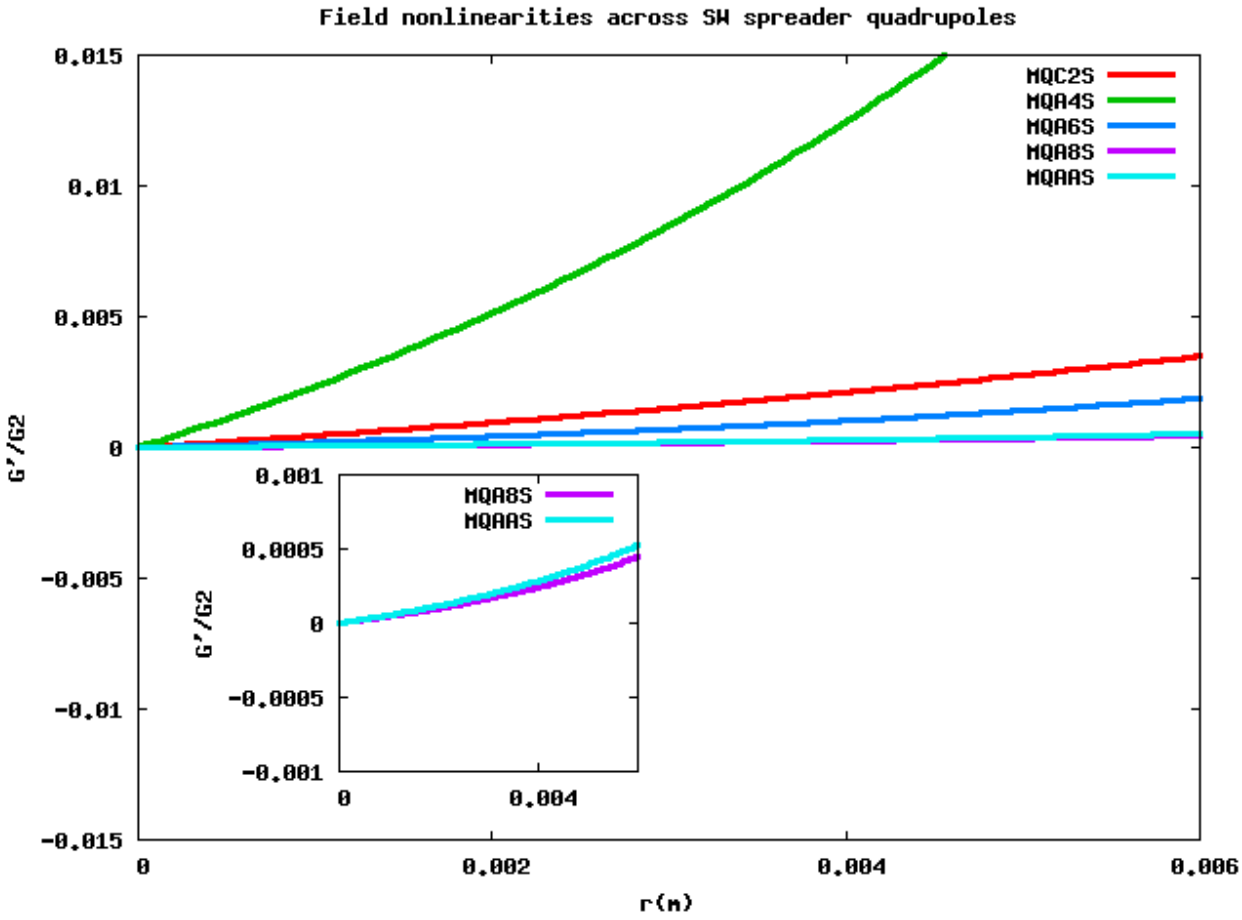

Figure 16: G'/G2 ratio across SW spreader quadrupoles

section	quad type	$\sqrt{\frac{1}{2}\sum_{n=1}^{N}\beta_n^2}$ [cm]	$\Delta\phi_1$ [cm^{-1}]	ϕ_1^{max} [cm^{-1}]	$\Delta\phi_1/\phi_1^{max}$	ε_x [cm rad]	$\left(\frac{\sigma_\varepsilon}{\varepsilon}\right)_{dil}$	$\Delta\phi_2$ [cm^{-2}]	$\Delta\phi_3$ [cm^{-3}]	$\Delta\phi_5$ [cm^{-5}]	$\Delta\phi_9$ [cm^{-9}]
Arc1	MQB	10298	6.9E-06	3.2E-03	2.2E-03	4.0E-08	0.467	6.2E-05	2.3E-05	3.2E-06	5.9E-08
Arc2	MQC	13515	5.2E-06	3.7E-03	1.4E-03	3.0E-08	0.374	3.8E-05	1.4E-05	1.9E-06	3.7E-08
Arc3	MQA	13320	5.3E-06	3.1E-03	1.7E-03	2.0E-08	0.457	5.7E-05	4.0E-05	1.9E-05	4.6E-06
Arc4	MQA	14392	4.9E-06	3.0E-03	1.7E-03	2.0E-08	0.468	5.2E-05	3.6E-05	1.8E-05	4.2E-06
Arc5	MQA	15036	4.7E-06	3.2E-03	1.5E-03	3.0E-08	0.296	2.5E-05	1.8E-05	8.6E-06	2.0E-06
Arc6	MQA	9376	7.5E-06	3.1E-03	2.5E-03	7.0E-08	0.134	1.6E-05	1.1E-05	5.5E-06	1.3E-06
Arc7	MQA	10380	6.8E-06	3.3E-03	2.1E-03	1.2E-07	0.100	8.1E-06	5.7E-06	2.8E-06	6.6E-07
Arc8	MQA	9585	7.4E-06	3.1E-03	2.4E-03	1.9E-07	0.100	7.1E-06	4.9E-06	2.4E-06	5.8E-07
Arc9	MQA	10424	6.8E-06	3.3E-03	2.1E-03	3.6E-07	0.100	4.6E-06	3.2E-06	1.6E-06	3.8E-07
ArcA	MQA	10439	6.8E-06	3.3E-03	2.1E-03	5.0E-07	0.100	3.9E-06	2.7E-06	1.3E-06	3.2E-07

Table 7: Calculated multipoles for arc quadrupoles

section	quad type	$\sqrt{\frac{1}{2}\sum_{n=1}^{N}\beta_n^2}$ [cm]	$\Delta\phi_1$ [cm^{-1}]	ϕ_1^{max} [cm^{-1}]	$\Delta\phi_1/\phi_1^{max}$	ε_x [cm rad]	$\left(\frac{\sigma_\varepsilon}{\varepsilon}\right)_{dil}$	$\Delta\phi_2$ [cm^{-2}]	$\Delta\phi_3$ [cm^{-3}]	$\Delta\phi_5$ [cm^{-5}]	$\Delta\phi_9$ [cm^{-9}]
Spr/Rec 1	MQB	10965	9.1E-06	4.4E-03	2.1E-03	4.0E-08	0.467	5.6E-05	2.1E-05	2.8E-06	5.3E-08
Spr/Rec 2	MQC	24773	4.0E-06	7.5E-03	5.4E-04	3.0E-08	0.374	1.6E-05	5.9E-06	8.2E-07	1.5E-08
Spr/Rec 3	MQA	20257	4.9E-06	4.9E-03	1.0E-03	2.0E-08	0.457	3.1E-05	2.1E-05	1.0E-05	2.5E-06
Spr/Rec 4	MQA	12599	7.9E-06	5.8E-03	1.4E-03	2.0E-08	0.468	6.1E-05	4.3E-05	2.1E-05	5.0E-06
Spr/Rec 5	MQA	13661	7.3E-06	5.5E-03	1.3E-03	3.0E-08	0.296	2.9E-05	2.0E-05	1.0E-05	2.4E-06
Spr/Rec 6	MQA	14853	6.7E-06	5.9E-03	1.1E-03	7.0E-08	0.134	5.1E-06	3.5E-06	1.7E-06	4.1E-07
Spr/Rec 7	MQA	26139	3.8E-06	5.6E-03	6.8E-04	1.2E-07	0.100	1.8E-06	1.3E-06	6.3E-07	1.5E-07
Spr/Rec 8	MQA	36216	2.8E-06	4.7E-03	5.9E-04	1.9E-07	0.100	9.5E-07	6.7E-07	3.3E-07	7.8E-08
Spr/Rec 9	MQA	22897	4.4E-06	2.1E-03	2.1E-03	3.6E-07	0.100	1.1E-06	7.8E-07	3.8E-07	9.1E-08
Spr/Rec A	MQA	21686	4.6E-06	4.6E-03	1.0E-03	5.0E-07	0.100	1.1E-06	7.7E-07	3.8E-07	9.0E-08

Table 8: Calculated multipoles across spreaders and recombiners quadrupoles

section	dipole type	$\sqrt{\frac{1}{2}\sum_{n=1}^{N}\beta_n^2}$ [cm]	$\Delta\phi_1$ [cm^{-1}]	$\Delta\phi_1 / \phi_1^{max}$	ε_x [cm rad]	$\left(\frac{\sigma_\varepsilon}{\varepsilon}\right)_{dil}$	$\Delta\phi_2$ [cm^{-2}]	$\Delta\phi_4$ [cm^{-4}]
Arc1	MBE	5664	1.2E-05	3.9E-03	4.0E-08	0.467	8.1E-04	5.0E-04
Arc2	MBR	7052	1.0E-05	2.7E-03	3.0E-08	0.374	5.4E-04	3.4E-04
Arc3	MBE	8072	8.8E-06	2.9E-03	2.0E-08	0.457	8.0E-04	5.0E-04
Arc4	MBB	8292	8.5E-06	2.9E-03	2.0E-08	0.468	8.0E-04	5.0E-04
Arc5	MBB	8667	8.2E-06	2.6E-03	3.0E-08	0.296	3.9E-04	2.4E-04
Arc6	MBB	6732	1.1E-05	3.4E-03	7.0E-08	0.134	1.8E-04	1.1E-04
Arc7	MBA	8191	8.6E-06	2.7E-03	1.2E-07	0.100	7.6E-05	4.7E-05
Arc8	MBA	6655	1.1E-05	3.5E-03	1.9E-07	0.100	8.0E-05	5.0E-05
Arc9	MBA	8188	8.6E-06	2.7E-03	3.6E-07	0.100	4.3E-05	2.7E-05
ArcA	MBA	8207	8.6E-06	2.6E-03	5.0E-07	0.100	3.7E-05	2.3E-05

Table 9: Calculated multipoles across arc dipoles

section	$\sqrt{\frac{1}{2}\sum_{n=1}^{N}\beta_n^2}$ [cm]	$\Delta\phi_1\left[cm^{-1}\right]$	$\Delta\phi_1 / \phi_1^{max}$	ε_x [cm rad]	$\left(\frac{\sigma_\varepsilon}{\varepsilon}\right)_{dil}$	$\Delta\phi_2$ [cm^{-2}]	$\Delta\phi_4$ [cm^{-4}]
Spr/Rec 1	3739	2.7E-05	6.1E-03	4.0E-08	0.467	1.5E-03	9.0E-04
Spr/Rec 2	8269	1.2E-05	1.6E-03	3.0E-08	0.374	4.0E-04	2.5E-04
Spr/Rec 3	8872	1.1E-05	2.3E-03	2.0E-08	0.457	5.8E-04	3.6E-04
Spr/Rec 4	14561	6.9E-06	1.2E-03	2.0E-08	0.468	3.1E-04	1.9E-04
Spr/Rec 5	9892	1.0E-05	1.8E-03	3.0E-08	0.296	2.5E-04	1.5E-04
Spr/Rec 6	16080	6.2E-06	1.1E-03	7.0E-08	0.134	3.9E-05	2.4E-05
Spr/Rec 7	19917	5.0E-06	9.0E-04	1.2E-07	0.100	1.4E-05	8.8E-06
Spr/Rec 8	18628	5.4E-06	1.2E-03	1.9E-07	0.100	1.3E-05	8.0E-06
Spr/Rec 9	36192	2.8E-06	1.3E-03	3.6E-07	0.100	3.1E-06	1.9E-06
Spr/Rec A	26014	3.8E-06	8.4E-04	5.0E-07	0.100	4.4E-06	2.7E-06

Table 10: Calculated multipoles across spreader and recombiner dipoles